BMC Medical Imaging

RESEARCH

Open Access

Radiomics based on MRI to predict recurrent L4-5 disc herniation after percutaneous endoscopic lumbar discectomy

Antao Lin[1†], Hao Zhang[1†], Yan Wang[1], Qian Cui[2], Kai Zhu[1], Dan Zhou[1], Shuo Han[1], Shengwei Meng[1], Jialuo Han[1], Lei Li[1], Chuanli Zhou[1*] and Xuexiao Ma[1*]

Abstract

Background In recent years, radiomics has been shown to be an effective tool for the diagnosis and prediction of diseases. Existing evidence suggests that imaging features play a key role in predicting the recurrence of lumbar disk herniation (rLDH). Thus, this study aimed to evaluate the risk of rLDH in patients undergoing percutaneous endoscopic lumbar discectomy (PELD) using radiomics to facilitate the development of more rational surgical and perioperative management strategies.

Method This was a retrospective case-control study involving 487 patients who underwent PELD at the L4/5 level. The rLDH and negative groups were matched using propensity score matching (PSM). A total of 1409 radiomic features were extracted from preoperative lumbar MRI images using intraclass correlation coefficient (ICC) analysis, t-test, and LASSO analysis. Afterward, 6 predictive models were constructed and evaluated using ROC curve analysis, AUC, specificity, sensitivity, confusion matrix, and 2 repeated 3-fold cross-validations. Lastly, the Shapley Additive Explanation (SHAP) analysis provided visual explanations for the models.

Results Following screening and matching, 128 patients were included in both the recurrence and control groups. Moreover, 18 of the extracted radiomic features were selected for generating six models, which achieved an AUC of 0.551–0.859 for predicting rLDH. Among these models, SVM, RF, and XG Boost exhibited superior performances. Finally, cross-validation revealed that their accuracy was 0.674–0.791, 0.647–0.729, and 0.674–0.718.

Conclusion Radiomics based on MRI can be used to predict the risk of rLDH, offering more comprehensive guidance for perioperative treatment by extracting imaging information that cannot be visualized with the naked eye. Meanwhile, the accuracy and generalizability of the model can be improved in the future by incorporating more data and conducting multicenter studies.

Keywords Intervertebral disc displacement, Endoscopes, Diskectomy, Recurrence, Radiomics

†Antao Lin and Hao Zhang contributed equally to this work.

*Correspondence:
Chuanli Zhou
justin_5257@hotmail.com
Xuexiao Ma
maxuexiaospinal@163.com

[1]Department of Spinal Surgery, The Affiliated Hospital of Qingdao University, No.59 Haier Road, Qingdao, Shandong 266000, People's Republic of China
[2]Department of Medical Imaging, The Affiliated Hospital of Qingdao University, Qingdao, Shandong, People's Republic of China

Introduction

At present, percutaneous endoscopic lumbar discectomy (PELD) is considered a popular minimally invasive technique in spine surgery. Indeed, it is widely adopted by surgeons and patients owing to the advantages of being non-traumatic, involving minimal bleeding, and allowing for faster recovery compared with traditional spine surgery [1, 2]. However, the remaining portion of the disc puts patients at risk for recurrence of lumbar disc herniation (rLDH), with reported incidence rates ranging from 2.8 to 15% [3–5]. Therefore, there is a pressing need to preoperatively evaluate the risk of recurrence to inform individualized management during the perioperative period.

Currently, radiomics is extensively applied in the field of skeletal muscle systems for bone tumors, such as differential diagnosis of bone diseases and tumors, prediction of tumor complications, prognosis of tumor treatment, and pathological grading [6–8]. While studies related to radiomics for osteoporosis have also surged in recent years [9], research investigating LHD remains scarce.

With advances in radiological techniques, radiological imaging has emerged as a crucial examination in spine surgery, with lumbar MR being the most important imaging examination for lumbar disc herniation. As is well documented, imaging features play a pivotal role in the early prediction and prevention of rLDH. Nonetheless, these features have not been systematically and comprehensively analyzed [10]. Radiomic features, a large set of quantitative features mathematically extracted from medical images that reflect intra-regional heterogeneity, have been speculated to potentially provide unknown information related to specific diseases [11–14]. Therefore, this study aimed to preoperatively evaluate the risk of rLDH in patients undergoing PELD using radiomics techniques, thereby laying a theoretical reference for perioperative management.

Earlier studies have established that biomechanical performance varies at each lumbar disc level [15], with the incidence of rLDH in the L4/5 segment being relatively higher than in other levels [16, 17]. Therefore, this retrospective case-control study examined patients who underwent PELD at the L4/5 level.

Patients and methods

Study population and groups

This retrospective study was conducted on patients who underwent PELD for L4-5 disc herniation in our department. All radiological and relevant clinical data during the follow-up period were acquired from the clinical database of our medical institution. Between January 2014 and December 2022, a total of 3345 patients underwent PELD at the L4/5 level, of which 487 patients were followed up and had complete data.

Following a thorough review of the clinical data of these patients, the inclusion and exclusion criteria were established as follows:

Inclusion criteria

(1) Patients who underwent PELD at the L4/5 segment; (2) Postoperative imaging displaying satisfactory decompression of the nerve; (3) Patients had an asymptomatic period of at least 2 weeks postoperatively, followed by recurrence of disc herniation at the same segment; (4) Postoperative follow-up for at least 1 year.

Exclusion criteria

(1) Patients with poor post-operative recovery and follow-up imaging data displaying persistent nerve compression (surgery-related); (2) Disc herniation at segments other than L4/5; (3) Comorbid thoracolumbar spine diseases (e.g., spinal fractures, infections, compulsory spondylitis, rheumatoid arthritis, tumors, etc.); (4) Previous surgeries within 3 adjacent segments.

According to the criteria described in previous studies [17], recurrent lumbar disc herniation (rLDH) was defined as follows: (1) Recurrence of neuropathic lower extremity pain after a postoperative asymptomatic period of at least 2 weeks; (2) Sagittal and transverse T2WI sequences of repeat MRI depicting protrusion of the nucleus pulposus from the L4/5 intervertebral space into the spinal canal or intervertebral foramen, accompanied by compression and deformation of the dural sac. Participants who experienced rLDH in this study underwent reoperation.

Considering the large difference in numbers and internal variability between the two groups, propensity score matching (PSM) was performed. Five variables were matched using PSM, namely gender, BMI, height, weight, and age, using a 1:1 matching protocol (nearest-matching algorithm), with a caliper width of 0.2 times the standard deviation of the logit of the propensity score. Eventually, an equal number of rLDH cases were matched to nLDH patients. (Fig. 1)

MRI examination

MRI data were acquired using a 3.0T system (SIGNA Pioneer, GE Healthcare) equipped with a 32-channel thoracolumbar spine coil. Only sagittal sequences were used in this study due to the possibility of overlapping intervertebral discs with bone in the cross-sectional images, which can compromise the representativeness of images. Imaging parameters included: sagittal T2WI FRFSE sequence (TR 2394 ms and TE 120 ms); slice thickness of 4–5 mm, slice spacing of 0.8–1 mm, a field of view of 26*26 cm, matrix size of 320*256, and a total of 11 scanned slices.

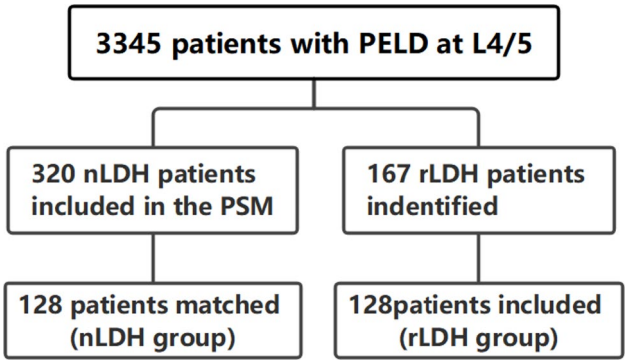

Fig. 1 Flow chart of patient inclusion and exclusion

Radiomic feature extraction and selection

All images were collected from the institution's Picture Archiving and Communication System (PACS) in DICOM format, with accordant window width and window location.

The region of interest (ROI) was manually outlined on T2WI using 3D Slicer software. In addition to the disc, its surrounding structures are also involved in the recurrence of disc herniation. Meng Kong and Chong Zhao identified lumbar lordosis, retrolisthesis, Modic changes, small muscle-disc ratio (M/D), and fatty infiltration as risk factors for PELD recurrence [10, 18]. Thus, the outlined area included the L4/5 disc and the two adjacent vertebral bodies, as well as the anterior half of the accessory pedicle, the anterior longitudinal ligament, and the posterior longitudinal ligament. (Fig. 2) Based on the defined ROI, 1409 features (including first-order statistics, shape-based 2d and 3d features, gray-level matrix, and wavelet-based features) were automatically extracted from the lumbar MRI using Python's pyradiomics package [19].

The intraclass correlation coefficient (ICC) was used to examine interobserver variability. A total of 36 patients were randomly selected for evaluation. The first author (Antao Lin) outlined the ROI and extracted the imaging features, following which co-author (Hao Zhang) independently repeated the outlining and extraction process. The two observers were blinded to the clinical information at the time of measurement. Radiomic features with ICC>0.75 were considered reliable and selected for the ensuing analyses.

Feature screening was conducted prior to the construction of the radiomics models, thereby minimizing overfitting or other types of bias. The t-test was used to compare the correlation of features between groups. Features with p-value<0.05 were considered significantly different and selected. Then, the least absolute shrinkage and selection operator (LASSO) analysis was employed to identify the ideal feature set. This approach reduced the coefficients of some features to zero via regularization, and the remaining features were used to construct the final model. Ten-fold cross-validation was used to adjust the regularization parameter (λ).

Establishment and evaluation of the predictive model

In the present study, six machine learning models were selected to predict lumbar disc herniation recurrence after PELD. These predictive models were developed using Python and included logistic regression (LR), support vector machine (SVM), Naive Bayes (NB), XG Boost (XGB), Random Forest (RF), and K-nearest Neighbor (kNN). The radiomic score (Rad score) was calculated for each patient using the following formula: Rad score $=\sum_{i=0}^{n} \mathrm{Ci}\times\mathrm{Xi} + \mathrm{b}$, where Xi represents the ith selected feature, Ci denotes the corresponding feature coefficient, and b is the intercept.

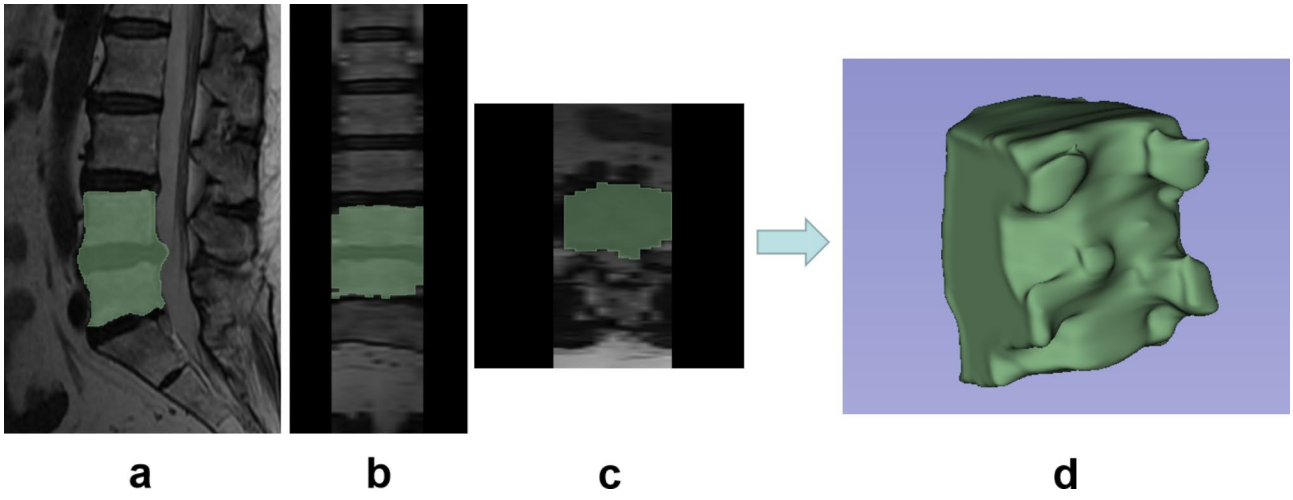

Fig. 2 The region of interest (ROI). The green area represents ROI. **a**: Sagittal position; **b**: Coronal position; **c**: Axis position; **d**: 3D rendering of ROI

Table 1 Before propensity score matching

	Non-rLDH	rLDH	*p*-value
n	320	128	
Group (%)			
0	320 (100)	0 (0)	< 0.001
1	0 (0)	128 (100)	
Gender (%)			
Female	129 (40.3)	48 (37.5)	0.658
Male	191 (59.7)	80 (62.5)	
BMI (mean (SD))	21.68 (3.78)	26.28 (3.23)	< 0.001
Height (mean (SD))	167.98 (8.48)	168.32 (8.09)	0.698
Weight (mean (SD))	61.25 (12.06)	74.66 (11.84)	< 0.001
Age (mean (SD))	55.02 (19.05)	59.43 (14.19)	0.018 (< 0.05)

rLDH: recurrence of lumbar disc herniation

Thereafter, patients were divided into a training set and a test set in the ratio of 7:3. The training set was used to develop the predictive model, whereas the test set was used to evaluate its performance. The receiver operating characteristic (ROC) curve was plotted using GraphPad Prism software. The performance of the model was evaluated by the area under the curve (AUC), and the DeLong test was performed to compare AUCs. Moreover, confusion matrices were plotted for models with superior predictive performance, and 2 repeated 3-fold cross-validation was performed for further evaluation.

Model interpretation

The application of machine learning techniques has traditionally been limited by challenges in interpreting their results. SHAP, proposed by Lundberg et al., is a game-theoretic approach that can be used to interpret machine learning models [20]. Specifically, the importance of each feature in the model can be ranked according to its SHAP value, and the summary plots of SHAP values can visually reflect the influence of each feature parameter on the results of the model's prediction.

Statistical analysis

R Studio, Python based on Anaconda, and 3D Slicer were used in this study. In R, PSM was performed using the MatchIt library, as listed in Appendix A. The chi-squared test or Fisher's exact test was used to compare categorical variables between two groups, and the t-test was used to compare continuous numerical variables. $p<0.05$ was considered statistically significant.

Results

Clinical characteristics

A total of 487 patients who underwent PELD for L4/5 disc herniation were recruited for this study. Based on clinical information and imaging, 167 of these patients developed rLDH. Patients with rLDH were further screened for completeness of follow-up data, and 128 patients who met the inclusion criteria and had complete data were finally included. Table 1 lists the demographic and clinical characteristics of the patients, with significant differences in BMI, age, and weight between the two groups ($p<0.05$). PSM was conducted to match the nLDH group to the rLDH group in a 1:1 ratio, with 128 individuals in the nLDH group matched to patients in the rLDH group. As anticipated, age, BMI, height, and weight were comparable between the matched groups. (Fig. 3; Table 2)

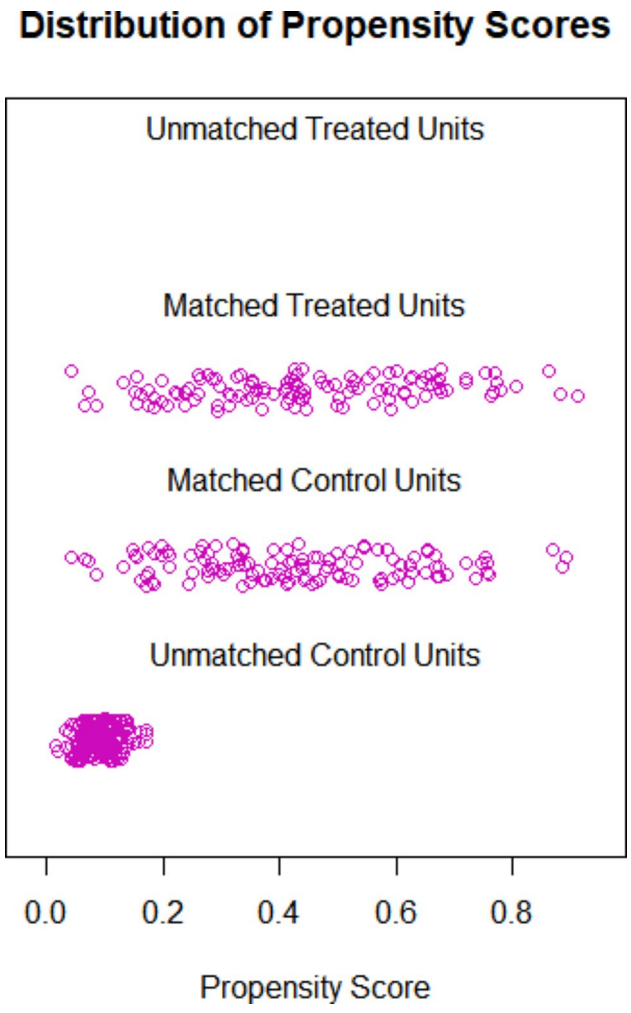

Fig. 3 Distribution of Propensity Scores

Radiomic features selection

A total of 1409 radiomics features were initially extracted from lumbar MRI images. Among them, 1318 features with ICC > 0.75 were selected. Observer 1 performed segmentation and radiomics extraction for all samples. Next, the selected 1318 features were tested for between-group differences using the t-test, and 140 features with a p-value < 0.05 were retained. Finally, the remaining features were further filtered using the LASSO analysis. Ten-fold cross-validation was used to select the optimal

Table 2 After propensity score matching

	Non-rLDH	rLDH	*p*-value
n	128	128	
Group (%)			
0	128 (100)	0 (0)	< 0.001
1	0 (0)	128 (100)	
Gender (%)			
Female	43 (33.6)	48 (37.5)	0.601
Male	85 (66.4)	80 (62.5)	
BMI (mean (SD))	25.55 (3.72)	26.28 (3.23)	0.805
Height (mean (SD))	167.46 (8.80)	168.32 (8.09)	0.732
Weight (mean (SD))	71.89 (13.29)	74.66 (11.84)	0.935
Age (mean (SD))	55.37 (16.36)	59.43 (14.19)	0.888

rLDH: recurrence of lumbar disc herniation

tuning parameter (λ) in the LASSO analysis, which was found to be 0.023 (Fig. 4). Finally, 18 features were incorporated into the radiomics models. (Table 3)

Predictive model construction and evaluation

The ROC curves, AUC, and 95% confidence intervals for the six predictive models are illustrated in Fig. 5. Based on the ROC curves and the results of the DeLong test, the RF, SVM, and XGB models outperformed the KNN, NB, and LR models in predicting lumbar disc herniation recurrence. Meanwhile, the specificity, sensitivity, Youden index, and cut-off value of the six predictive models were also calculated. (Tables 4 and 5) Then, the confusion matrices for RF, SVM, and XG Boost displayed ideal prediction performance. (Fig. 6) Finally, repeated 3-fold cross-validation was carried out twice to evaluate the performance of these three models and to prevent over-fitting. (Table 6)

Table 3 The 18 features chosen for the radiomics model by LASSO analysis

	Image type	Feature class	Feature name	LASSO coefficient (β)
1	original	shape	Elongation	-0.029618
2	original	shape	MinorAxisLength	-0.011353
3	exponential	glszm	LargeAreaHighGrayLevelEmphasis	-0.033109
4	gradient	glcm	Correlation	0.032793
5	gradient	glcm	MCC	0.055625
6	lbp-2D	gldm	SmallDependenceEmphasis	0.020327
7	lbp-2D	glrlm	RunEntropy	-0.034613
8	lbp-2D	glrlm	RunLengthNonUniformity	0.119266
9	square	glcm	Idn	0.048664
10	square	ngtdm	Strength	0.004756
11	squareroot	glcm	Idmn	0.026030
12	squareroot	glcm	Idn	0.003533
13	wavelet-LHH	first-order	Kurtosis	-0.024043
14	wavelet-LHH	glcm	MCC	-0.006359
15	wavelet-LHH	glszm	GrayLevelVariance	-0.048173
16	wavelet-HLH	first-order	Median	0.050614
17	wavelet-HHL	ngtdm	Strength	0.029183
18	wavelet-HHH	first-order	Kurtosis	-0.001111

Model interpretation

The SHAP summary plots for the RF, SVM, and XGB models are delineated in Fig. 7. The radiomic features were ranked in importance based on SHAP scores in the corresponding model, with the top 5 features presented in each figure. Each point in the figure represents an individual observation of the corresponding feature. Higher

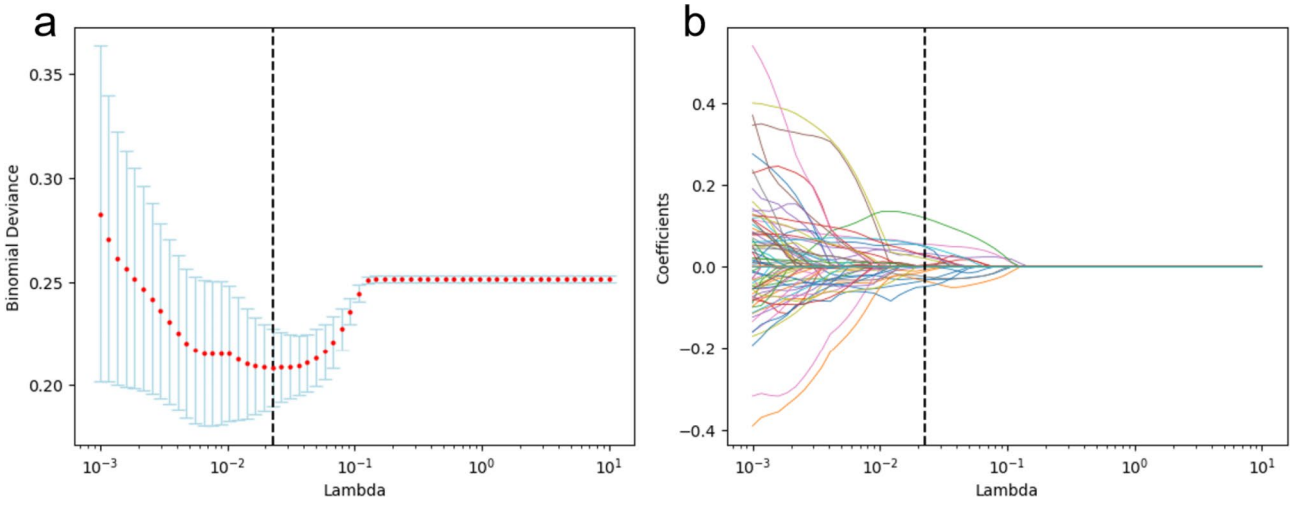

Fig. 4 LASSO analysis. **a**. Ten-fold cross-validation was used to select the uning parameter (λ) in the LASSO analysis. The y-axis correspond the binomial deviance while the x-axis correspond log (λ). The vertical dotted lines represented the minimum criteria. **b**.140 radiomic features coefficient profile versus the log (λ) sequence

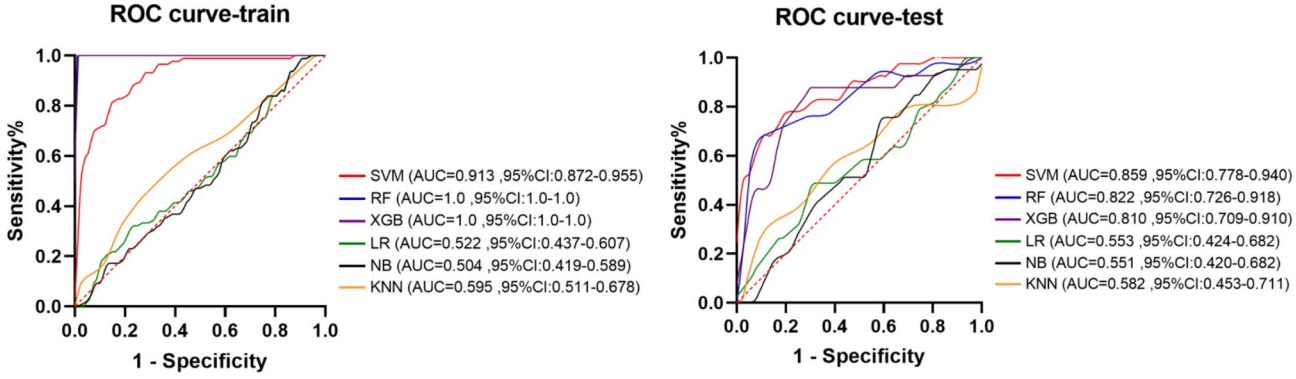

Fig. 5 ROC curve

Table 4 DeLong p-value of AUC

	XGB	KNN	LR	NB	RF	SVM
XGB	1	0.013	0.001	0.032	0.156	0.695
KNN	0.013	1	0.579	0.566	0.001	0.001
LR	0.001	0.579	1	0.283	0.000	0.000
NB	0.032	0.566	0.283	1	0.007	0.015
RF	0.156	0.001	0.000	0.007	1	0.754
SVM	0.695	0.001	0.000	0.015	0.754	1

XGB: XG Boost; KNN: K-nearest Neighbor; LR: Logistic Regression; NB: Naive Bayes; RF: Random Forest; SVM: Support Vector Machine

Table 5 Test cohort

Model type	Specificity	Sensitivity	Youden index	Cut-Off value
RF	0.889	0.683	0.572	0.525
SVM	0.917	0.683	0.600	0.638
XGB	0.722	0.878	0.600	0.337
LR	0.722	0.463	0.185	0.486
KNN	0.889	0.293	0.182	0.569
NB	0.083	1	0.083	0

XGB: XG Boost; KNN: K-nearest Neighbor; LR: Logistic Regression; NB: Naive Bayes; RF: Random Forest; SVM: Support Vector Machine

SHAP values for a feature indicate a higher risk of postoperative recurrence. Red indicates high eigenvalues, purple indicates eigenvalues close to the overall mean, and blue indicates low eigenvalues.

Discussion

Relevant studies on the application of radiomics in the field of LDH are limited. Gang Yu et al. retrospectively categorized patients with LDH who had achieved a definite therapeutic effect into two groups according to the treatment modality and constructed a nomogram-based predictive model by extracting pre-treatment MRI data of patients in the two groups through radiomics to predict the need for surgical intervention. The result suggested that the radiomics-based nomogram had a high predictive value for LDH treatment and could serve as a reference for clinical decision-making [21]. At the same time, Babak Saravi et al. incorporated features extracted from radiomics techniques with general clinical data to construct a predictive model of LDH surgical outcomes and reported a minimal but detectable improvement in predictive accuracy following the introduction of radiomics features in the model [22]. These studies conjointly highlight the value of radiomics in the diagnosis and treatment of LDH-related conditions.

This study investigated recurrence after percutaneous endoscopic lumbar discectomy to construct a predictive model for the risk of postoperative recurrence based on radiomics and the preoperative lumbar spine MRI data of patients with recurrent lumbar disc herniation using various machine learning tools to assess the risk of postoperative recurrence prior to percutaneous endoscopic lumbar discectomy and guide the formulation of individualized surgical and postoperative management strategies.

Herein, 1040 radiomic features were screened, yielding 18 features with a significant impact on predictive accuracy. While some of these features may be independently associated with rLDH, it is challenging to rely on a single feature for diagnosis [23]. Therefore, developing a multifeature model is a more robust approach [20]. Among the selected 18 features, 3 were first-order features, 2 were shape-based features, 6 were GLSZM, 2 were GLSZM, 2 were GLRLM, 2 were NGTDM, and 1 was GLDM [19]. This distribution signified that first-order and shape-based features easily identified by the naked eye are suboptimal for predicting the recurrence of lumbar disc herniation and should be combined with high-dimensional features that are not easily identified by the naked

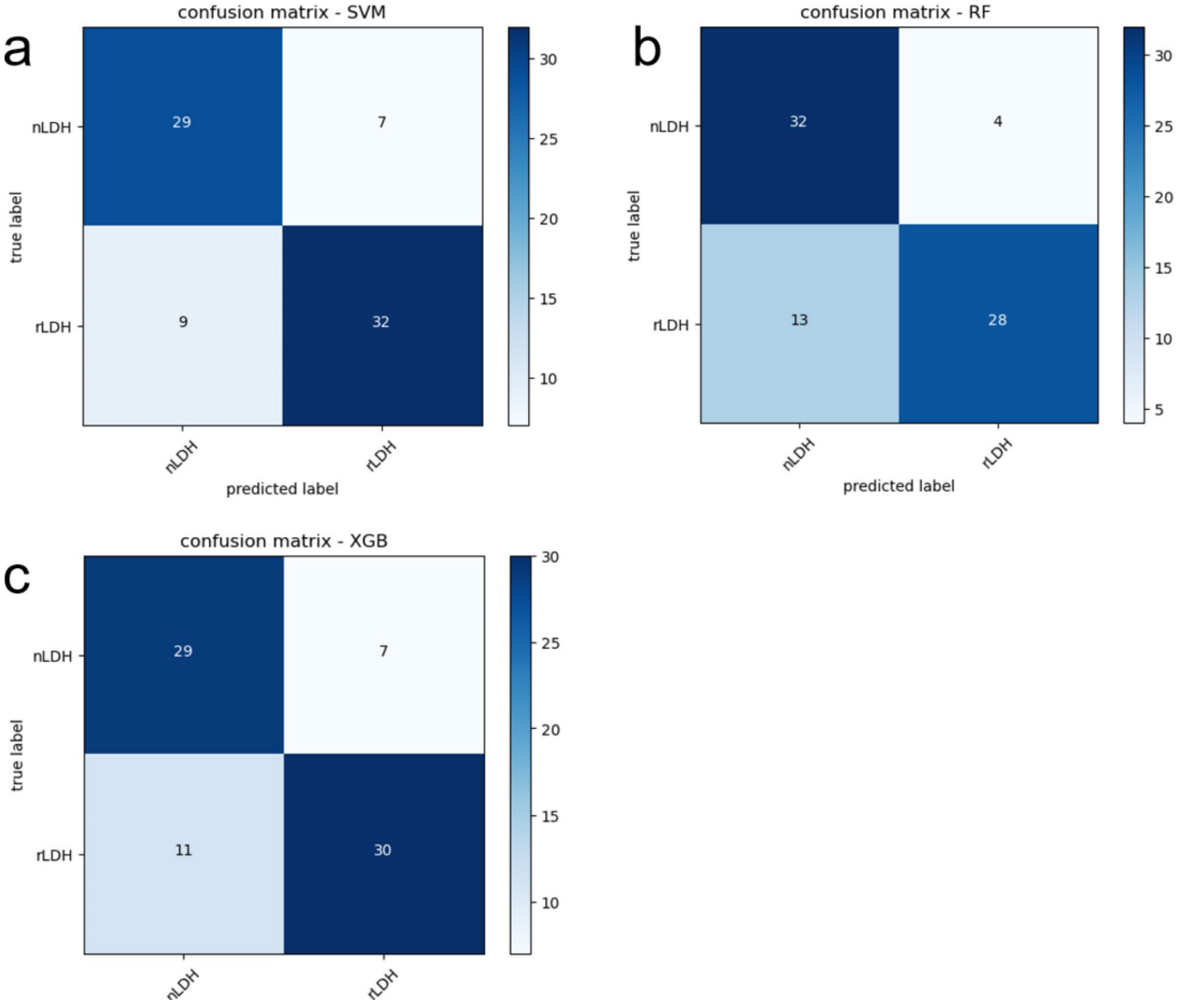

Fig. 6 Confusion Matrix of SVM, RF and XGB (test cohort). **a**. confusion matrix of support vector machine model; **b**. confusion matrix of random forest; **c**. confusion matrix of XG Boost

Table 6 The p-time and k-fold cross-validation accuracies ($p=2$, $k=3$) of the three predictive models

Model	XG Boost	RF	SVM
k-fold accuracy	0.709, 0.706, 0.682, 0.674, 0.718, 0.718	0.674, 0.647,0.729, 0.686, 0.706, 0.706	0.791, 0.682, 0.718, 0.674, 0.765, 0.753
Average	0.701	0.691	0.731
Standard deviation	0.019	0.029	0.047

XGB: XG Boost; RF: Random Forest; SVM: Support Vector Machine

eye. Overall, the 18 quantitative radiomic features identified in this study can offer additional information from lumbar disc herniation images.

Six predictive models were generated based on preoperative lumbar MRI images, and their AUC, specificity, and sensitivity were determined. The results of the Delong test exposed that the predictive performance of XGB, RF, and SVM was significantly higher compared to KNN, LR, and NB in the test set. Nevertheless, no significant differences in AUC were noted between the three high-performing models (Table 4, Fig. 5 and 6). Two repeated 3-fold cross-validations for these models unveiled that the SVM had the highest average accuracy of 0.731, whereas the XGB model demonstrated superior stability with a standard deviation of 0.019. (Table 6) To increase the interpretability of the predictive models,

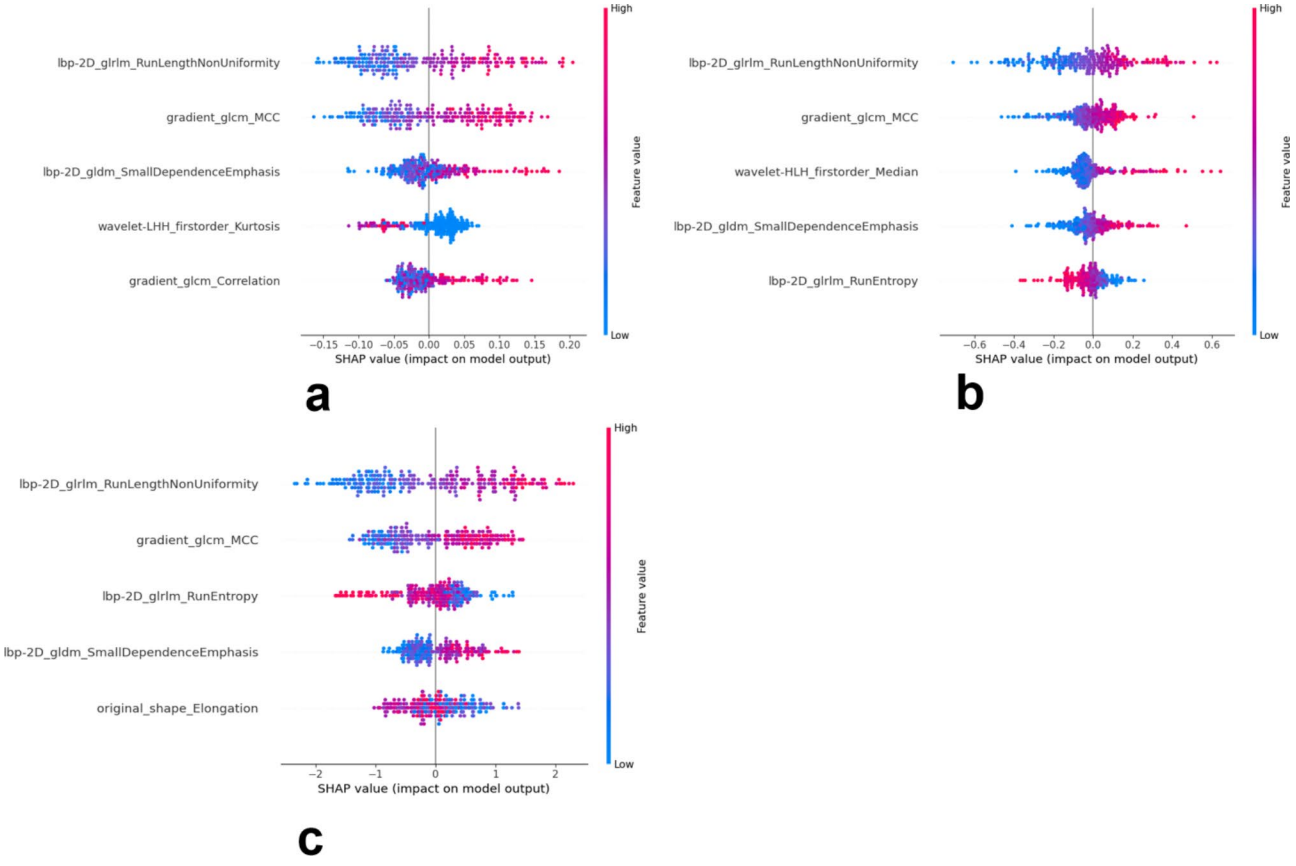

Fig. 7 The summary plots for SHAP values. **a**. The SHAP value of RF; **b**. the SHAP value of SVM; **c**. the SHAP value of XGB. (RF: random forest model; SVM: support vector machine model; XGB: XG Boost model)

SHAP analysis was performed to identify and depict the five most important radiomic features of each model to illustrate the mechanism by which these features influence predictive outcomes. (Fig. 7)

The Schulthess Klinik orthopedic team in Zurich, Switzerland, developed a predictive model for surgical outcomes through correlation regression analysis of factors such as baseline clinical data and postoperative pain scores in patients undergoing conventional lumbar decompression surgery. Notably, it can be used to predict the prognosis of conventional decompression surgery for lumbar disc herniation and to assist in clinical management [24]. Our results suggested that radiomic-based predictive models can be used as preoperative assessment tools to assess the risk of recurrence in preoperative patients, thereby informing clinical treatment decisions.

Regarding recurrence after PELD, Meng Kong et al. proposed several methods to minimize the risk of recurrence for both surgeons and patients [18]. Based on our study, we propose the following recommendations for patients with a high risk of postoperative recurrence: For surgeons: (1) The appropriate surgical strategy should be developed preoperatively (Based on patient preference, fusion internal fixation of the lesioned segment may be considered; If only partial discectomy is performed, PEID should be prioritized to facilitate reoperation in case of recurrence); (2) More intensive preoperative examination and intraoperative manipulation are required to ensure complete excision of the herniated disc; (3) In younger patients, consideration should be given to suturing the annulus fibrosus. For patients, (1) The importance of lifestyle modifications, such as weight loss, smoking cessation, and active glycemic control, should be emphasized; (2) Maintaining proper spinal alignment by keeping back straight and abdominal muscles engaged to maintain a physiological curvature should be encouraged; (3) Moderate exercise of low back muscles should be promoted in the absence of significant discomfort after surgery.

Limitations

To begin, an in-depth analysis of subgroups (e.g., by age group) was not performed due to the limited number of rLDH patients. Future studies should be conducted to optimize model performance. Secondly, in order to enhance the sensitivity of the model for predicting the risk of rLDH, this study exclusively enrolled patients with rLDH experiencing severe symptoms who required reoperation, whilst patients with mild recurrence symptoms

who were managed conservatively were excluded. Thirdly, PELD typically comprises PEID and PETD, and their effect on recurrence primarily involves intraoperative destruction of local structures, which is closely related to the location of the herniated disc. Relevant factors have been adjusted for during the extraction of preoperative radiomic features. Nevertheless, individual analyses of the effect of PEID and PETD were not conducted in order to minimize internal confounders.

Conclusion

This study demonstrates that radiomic modeling based on preoperative lumbar MRI images can effectively predict the risk of recurrence in patients undergoing percutaneous endoscopic lumbar disc discectomy. Notably, the use of advanced computational techniques allows for the acquisition of detailed imaging features that cannot be observed with the naked eye, contributing to a more comprehensive preoperative assessment of the risk of recurrence in minimally invasive surgeries and providing valuable insights for the development of surgical and postoperative rehabilitation programs. This allows surgeons to identify patients at higher risk of recurrence and make timely preoperative adjustments to the perioperative management strategy, which may include consideration of intraoperative suturing of the fibrous ring and extending postoperative bed rest. While the accuracy of this model warrants optimization, the incorporation of additional patient data, MRI sequences, and CT images may improve the accuracy of the model. Multicenter studies are necessitated to improve the generalizability of the model.

Abbreviations

MRI	Magnetic Resonance Imaging
PELD	Percutaneous Endoscopic Lumbar Discectomy
rLDH	recurrence of Lumbar Disk Herniation
PSM	Propensity Score Matching
ICC	Intraclass Correlation Coefficient
LASSO	Least Absolute Shrinkage and Selection Operator
SHAP	Shapley Additive Explanation
ROI	Region Of Interest
AUC	Area Under the Curve
LR	Logistic Regression
SVM	Support Vector Machine
NB	Naive Bayes
XGB	XG Boost
RF	Random Forest
KNN	K-Nearest Neighbor

Supplementary Information

The online version contains supplementary material available at https://doi.org/10.1186/s12880-024-01450-x.

Supplementary Material 1: Appendix A: The used packages in R Studio and Python.

Acknowledgements

The authors are grateful to staff of the imaging department for their technical assistance and to the medical recorders who helped with patient data collection. We would also like to thank the editorial board of BMC medical imaging for reviewing and critiquing the manuscript to improve it.

Author contributions

All authors contributed significantly to this work. ATL wrote the main manuscript text, HZ and YW provided important theoretical guidance. QC assisted in providing image information, XXM and CLZ are responsible for this article, and others provided important data about this article.

Funding

This study has received funding by the Qingdao Science and Technology Benefit the People Demonstration Project (23-2-8-smjk-7-nsh) and the Natural Science Foundation of Shan Dong Province (ZR2021MH020). The funding bodies played no role in the design of the study and collection, analysis, and interpretation of data and in writing the manuscript.

Data availability

All data generated or analysed during this study are included in this published article [and its supplementary information files].

Declarations

Ethics approval and consent to participate

All procedures were approved by the ethics committee of the Affiliated Hospital of Qingdao University and approved number of IRB was QYFYWZLL27871. Written informed consent was received from all patients and/or their legal guardian(s) before the operation. And all experiments were performed in accordance with relevant guidelines and regulations.

Consent for publication

Not applicable.

Competing interests

The authors declare no competing interests.

Received: 17 October 2023 / Accepted: 1 October 2024
Published online: 10 October 2024

References

1. Kanno H, Aizawa T, Hahimoto K, Itoi E. Minimally invasive discectomy for lumbar disc herniation: current concepts, surgical techniques, and outcomes. Int Orthop. 2019;43:917–22. https://doi.org/10.1007/s00264-018-4256-5.
2. Choi KC, Kim J-S, Park C-K. Percutaneous endoscopic lumbar discectomy as an alternative to open lumbar microdiscectomy for large lumbar disc herniation. Pain Physician. 2016;19:E291–300.
3. Yin S, Du H, Yang W, Duan C, Feng C, Tao H. Prevalence of recurrent herniation following percutaneous endoscopic lumbar discectomy: a Meta-analysis. Pain Physician. 2018;21:337–50.
4. Yoon SM, Ahn S-S, Kim KH, Kim YD, Cho JH, Kim D-H. Comparative study of the outcomes of Percutaneous endoscopic lumbar discectomy and microscopic lumbar discectomy using the tubular Retractor System based on the VAS, ODI, and SF-36. Korean J Spine. 2012;9:215–22. https://doi.org/10.14245/kjs.2012.9.3.215.
5. Chuanli Z. Unique Complications of Percutaneous EndoscopicLumbar Discectomy and Percutaneous EndoscopicInterlaminar Discectomy. Pain Physician. 2018;1:E105–12. https://doi.org/10.36076/ppj.2018.2.E105.
6. Wang H, Chen H, Duan S, Hao D, Liu J. Radiomics and Machine Learning with Multiparametric Preoperative MRI May accurately predict the histopathological grades of soft tissue sarcomas. J Magn Reson Imaging JMRI. 2020;51:791–7. https://doi.org/10.1002/jmri.26901.
7. Zhang J, Sun J, Han T, Zhao Z, Cao Y, Zhang G, Zhou J. Radiomic features of magnetic resonance images as novel preoperative predictive factors of bone invasion in meningiomas. Eur J Radiol. 2020;132:109287. https://doi.org/10.1016/j.ejrad.2020.109287.
8. Pan J, Zhang K, Le H, Jiang Y, Li W, Geng Y, Li S, Hong G. Radiomics Nomograms based on non-enhanced MRI and clinical risk factors for the

differentiation of Chondrosarcoma from Enchondroma. J Magn Reson Imaging JMRI. 2021;54:1314–23. https://doi.org/10.1002/jmri.27690.
9. Jiang Y-W, Xu X-J, Wang R, Chen C-M. Radiomics analysis based on lumbar spine CT to detect osteoporosis. Eur Radiol. 2022;32:8019–26. https://doi.org/10.1007/s00330-022-08805-4.
10. Zhao C, Zhang H, Wang Y, Xu D, Han S, Meng S, Han J, Liu H, Zhou C, Ma X. Nomograms for Predicting recurrent herniation in PETD with preoperative radiological factors. J Pain Res. 2021;14:2095–109. https://doi.org/10.2147/JPR.S312224.
11. Lambin P, Rios-Velazquez E, Leijenaar R, Carvalho S, van Stiphout RGPM, Granton P, Zegers CML, Gillies R, Boellard R, Dekker A, Aerts HJWL. Radiomics: extracting more information from medical images using advanced feature analysis. Eur J Cancer Oxf Engl 1990. 2012;48:441–6. https://doi.org/10.1016/j.ejca.2011.11.036.
12. He L, Liu Z, Liu C, Gao Z, Ren Q, Lei L, Ren J. Radiomics Based on Lumbar Spine Magnetic Resonance Imaging to detect osteoporosis. Acad Radiol. 2021;28:e165–71. https://doi.org/10.1016/j.acra.2020.03.046.
13. Mu W, Jiang L, Zhang J, Shi Y, Gray JE, Tunali I, Gao C, Sun Y, Tian J, Zhao X, Sun X, Gillies RJ, Schabath MB. Non-invasive decision support for NSCLC treatment using PET/CT radiomics. Nat Commun. 2020;11:5228. https://doi.org/10.1038/s41467-020-19116-x.
14. Wang X, Wan Q, Chen H, Li Y, Li X. Classification of pulmonary lesion based on multiparametric MRI: utility of radiomics and comparison of machine learning methods. Eur Radiol. 2020;30:4595–605. https://doi.org/10.1007/s00330-020-06768-y.
15. Hasegawa K, Kitahara K, Hara T, Takano K, Shimoda H, Homma T. Evaluation of lumbar segmental instability in degenerative diseases by using a new intraoperative measurement system. J Neurosurg Spine. 2008;8:255–62. https://doi.org/10.3171/SPI/2008/8/3/255.
16. Suk KS, Lee HM, Moon SH, Kim NH. Recurrent lumbar disc herniation: results of operative management. Spine. 2001;26:672–6. https://doi.org/10.1097/00007632-200103150-00024.
17. Kim HS, You JD, Ju CI. Predictive scoring and risk factors of early recurrence after percutaneous endoscopic lumbar discectomy. BioMed Res Int. 2019;2019:6492675. https://doi.org/10.1155/2019/6492675.
18. Kong M, Xu D, Gao C, Zhu K, Han S, Zhang H, Zhou C, Ma X. Risk factors for recurrent L4-5 disc herniation after percutaneous endoscopic transforaminal discectomy: a retrospective analysis of 654 cases, risk Manag. Healthc Policy. 2020;13:3051–65. https://doi.org/10.2147/RMHP.S287976.
19. Zwanenburg A, Leger S, Vallières M, Löck S. Image biomarker standardisation initiative. Radiology. 2020;295:328–38. https://doi.org/10.1148/radiol.2020191145.
20. Lundberg S, Lee S-I, editors. A unified approach to interpreting model predictions., in: Proc. 31st Int. Conf. Neural Inf. Process. Syst., 2017.
21. Yu G, Yang W, Zhang J, Zhang Q, Zhou J, Hong Y, Luo J, Shi Q, Yang Z, Zhang K, Tu H. Application of a nomogram to radiomics labels in the treatment prediction scheme for lumbar disc herniation. BMC Med Imaging. 2022;22:51. https://doi.org/10.1186/s12880-022-00778-6.
22. Saravi B, Zink A, Ülkümen S, Couillard-Despres S, Wollborn J, Lang G, Hassel F. Clinical and radiomics feature-based outcome analysis in lumbar disc herniation surgery. BMC Musculoskelet Disord. 2023;24:791. https://doi.org/10.1186/s12891-023-06911-y.
23. Jiang Y, Chen C, Xie J, Wang W, Zha X, Lv W, Chen H, Hu Y, Li T, Yu J, Zhou Z, Xu Y, Li G. Radiomics signature of computed tomography imaging for prediction of survival and chemotherapeutic benefits in gastric cancer. EBioMedicine. 2018;36:171–82. https://doi.org/10.1016/j.ebiom.2018.09.007.
24. Staub LP, Aghayev E, Skrivankova V, Lord SJ, Haschtmann D, Mannion AF. Development and temporal validation of a prognostic model for 1-year clinical outcome after decompression surgery for lumbar disc herniation. Eur Spine J off Publ Eur Spine Soc Eur Spinal Deform Soc Eur Sect Cerv Spine Res Soc. 2020;29:1742–51. https://doi.org/10.1007/s00586-020-06351-5.

Publisher's note